Dynamic instability of marine-terminating glacier basins of Academy of Sciences Ice Cap, Russian High Arctic

Geir MOHOLDT,[1,2] Torborg HEID,[1] Toby BENHAM,[3] Julian A. DOWDESWELL[3]

[1]Department of Geosciences, University of Oslo, Oslo, Norway
E-mail: gmoholdt@ucsd.edu
[2]Institute of Geophysics and Planetary Physics, Scripps Institution of Oceanography, University of California, San Diego, La Jolla, CA, USA
[3]Scott Polar Research Institute, University of Cambridge, Cambridge, UK

ABSTRACT. Ice sheets and smaller ice caps appear to behave in dynamically similar ways; both contain slow-moving ice that is probably frozen to the bed, interspersed with fast-flowing ice streams and outlet glaciers that terminate into the ocean. Academy of Sciences Ice Cap (Akademii Nauk ice cap; 5570 km^2), Severnaya Zemlya, Russian High Arctic, provides a clear example of this varied flow regime. We have combined satellite measurements of elevation change and surface velocity to show that variable ice-stream dynamics dominate the mass balance of the ice cap. Since 1988, the ice cap has lost 58 ± 16 Gt of ice, corresponding to ~3% of its mass or 0.16 mm of sea-level rise. The climatic mass balance is estimated to be close to zero, and terminus positions have remained stable to within a few kilometers, implying that almost all mass loss has occurred through iceberg calving. The ice-cap calving rate increased from ~0.6 Gt a^{-1} in 1995 to ~3.0 Gt a^{-1} in 2000–02, but has recently decreased to ~1.4 Gt a^{-1} due to a likely slowdown of the largest ice stream. Such highly variable calving rates have not been reported before from High Arctic ice caps, suggesting that these ice masses may be less stable than previously thought.

INTRODUCTION

Recent studies have shown that marine-terminating glacier dynamics play a major role in the mass balance of outlet glaciers in Antarctica, Greenland and Alaska. Outlet glaciers on the Antarctic Peninsula have been observed to accelerate after break-up of buttressing ice shelves (Scambos and others, 2004), and warmer than usual ocean water is believed to be one of the main drivers for the recent retreat and acceleration of Greenland outlet glaciers (Holland and others, 2008). Marine glacier basins in Greenland are thinning about twice as fast as their land-terminating neighbors (Sole and others, 2008). This trend has so far not been observed for marine glaciers in the High Arctic archipelagos, although they experience comparable climatic and oceanic forcing (Gardner and others, 2011). In this study, we use measurements of changes in glacier area, velocity and surface elevation to infer glacier dynamics and calving rates for the largest ice cap in the Russian Arctic, Academy of Sciences Ice Cap.

Academy of Sciences Ice Cap, sometimes referred to as Akademii Nauk ice cap (Fritzsche and others, 2005), is located at 80.5° N, 95° E on Komsomolets island in the Severnaya Zemlya archipelago (Fig. 1). The region has a cold, dry climate with a mean annual air temperature of about –16°C (Bassford and others, 2006). Precipitation increases with altitude and has been measured to a long-term average of 0.46 m w.e. a^{-1} at the summit of Academy of Sciences Ice Cap (Fritzsche and others, 2005). Time series of in situ mass-balance measurements on Severnaya Zemlya exist only for Vavilov Ice Cap, on neighboring October Revolution Island (Fig. 1), over a limited number of years in the 1970s–80s. They indicate a slightly negative climatic mass balance (Bassford and others, 2006). Most iceberg calving in the region occurs from the Matusevitch Ice Shelf (Williams and Dowdeswell, 2001) and the fast-flowing ice

streams of Academy of Sciences Ice Cap. The total calving flux of Academy of Sciences Ice Cap has previously been estimated to be ~0.6 Gt a^{-1} (Dowdeswell and others, 2002), based on ice thicknesses from airborne radio-echo sounding and surface velocities from synthetic aperture radar (SAR) interferometry (Fig. 2). There is no evidence of past surge activity on Academy of Sciences Ice Cap and little for glaciers in Severnaya Zemlya more generally (Dowdeswell and Williams, 1997; Dowdeswell and others, 2002).

The morphology of Academy of Sciences Ice Cap is relatively simple, with a single dome that rises to an elevation of 750 m (Fig. 3a). Airborne radio-echo sounding shows that most of the north is grounded above sea level, while most of the southeast and west is grounded below sea level (Fig. 2a). In total, ~50% of the ice cap is grounded below sea level, and 200 km (50%) of the ice margin is marine. The total ice-cap volume is ~2200 km^3 (Dowdeswell and others, 2002).

SURFACE VELOCITIES AND DRAINAGE BASINS

Extraction of ice-surface velocities from satellite data is difficult in regions like Severnaya Zemlya due to frequent cloud cover and low visual contrast in optical imagery, as well as rapid temporal decorrelation of amplitude and phase in SAR acquisitions over snow and ice. The only semi-complete map of surface velocities on Academy of Sciences Ice Cap is from single-look SAR interferometry (InSAR) during the 1 day tandem phase of European Remote-sensing Satellites-1 and -2 (ERS-1/2) in 1995 (Dowdeswell and others, 2002). Surface deformation could only be detected in the satellite look direction (northeastward; Fig. 2b), and a digital elevation model (DEM) had to be used to decompose look-angle vectors into assumed downslope movement. This is only feasible for angles within ~70° of the look direction,
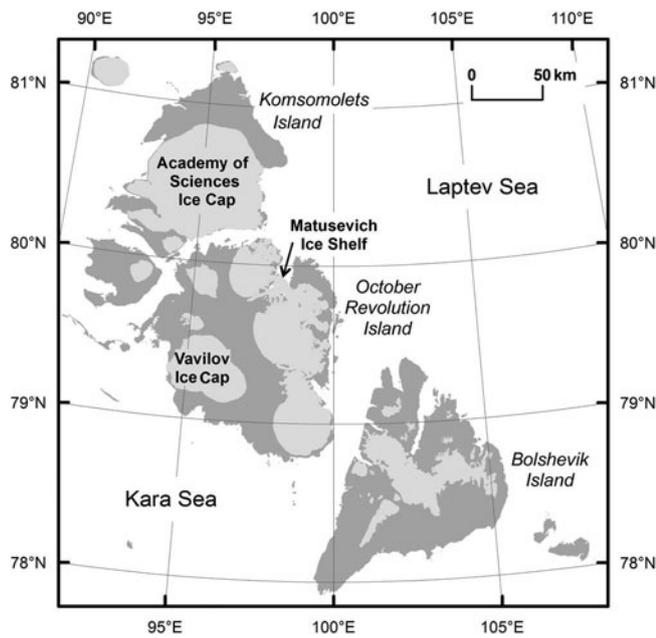
Fig. 1. Location of Academy of Sciences Ice Cap within the Severnaya Zemlya archipelago in the Russian High Arctic.

so potential perpendicular movements (i.e. southeast–northwest) could not be resolved. The derived surface velocity map shows four fast-flowing units that largely follow submarine bedrock troughs (Fig. 2). These units are referred to as ice streams A–D, and they form the basis for the separation of glacier drainage basins in Figure 3a. The drainage divides mapped in Figure 3a are consistent with Dowdeswell and others (2002), except for the northern edge of basin D which we moved southward to fit the observed extent of dynamic thinning (Fig. 4). The slow-moving ($<10\,m\,a^{-1}$) northern parts of the ice cap were combined into a single unit named basin north. The ice-cap outline was digitized from georeferenced Landsat imagery acquired on 5 June 2002 and 21 August 2010.

Little is known about temporal variations in surface velocity of Academy of Sciences Ice Cap. Multitemporal velocity data from an ice stream on Austfonna ice cap, northeastern Svalbard, show that motion can vary substantially on decadal, annual and seasonal timescales (Dowdeswell and others, 1999; Dunse and others, 2011b). In order to investigate possible variability, we undertook image matching between repeat-pass optical satellite imagery of Severnaya Zemlya. We used orientation correlation in the frequency domain (Fitch and others, 2002), a method that can derive ice displacements at sub-pixel accuracy (Haug and others, 2010; Heid and Kääb, 2012). We did not find any image pairs with short enough repeat times to provide consistent image character and thus allow spatially extensive image matching. Parts of the crevasse zones of ice streams B–D were matched between pairs of orthorectified Landsat scenes acquired at 1–2 year intervals between the summers of 2000 and 2002 (Fig. 3c and d). The average surface velocity and standard deviation within 5–10 km of the terminus was $725 \pm 61\,m\,a^{-1}$ for ice stream B, 583 ± 120 $m\,a^{-1}$ for ice stream C and $549 \pm 44\,m\,a^{-1}$ for ice stream D. These velocities are several times higher than the earlier InSAR velocities at similar locations (Fig. 2b). The Landsat velocities have the advantage that they are averaged over 1–2 years so that potential seasonal speed-ups are captured. The onset of the summer melt season has been shown to cause a twofold increase in surface velocities at a comparable fast-flowing ice stream on Austfonna ice cap (Dunse and others, 2011b). Such accelerations are, however, relatively short-lived and cannot explain the large difference between the two velocity datasets. We hypothesize that all three ice streams were in a more rapid phase of flow in 2000–02 than around 1995.
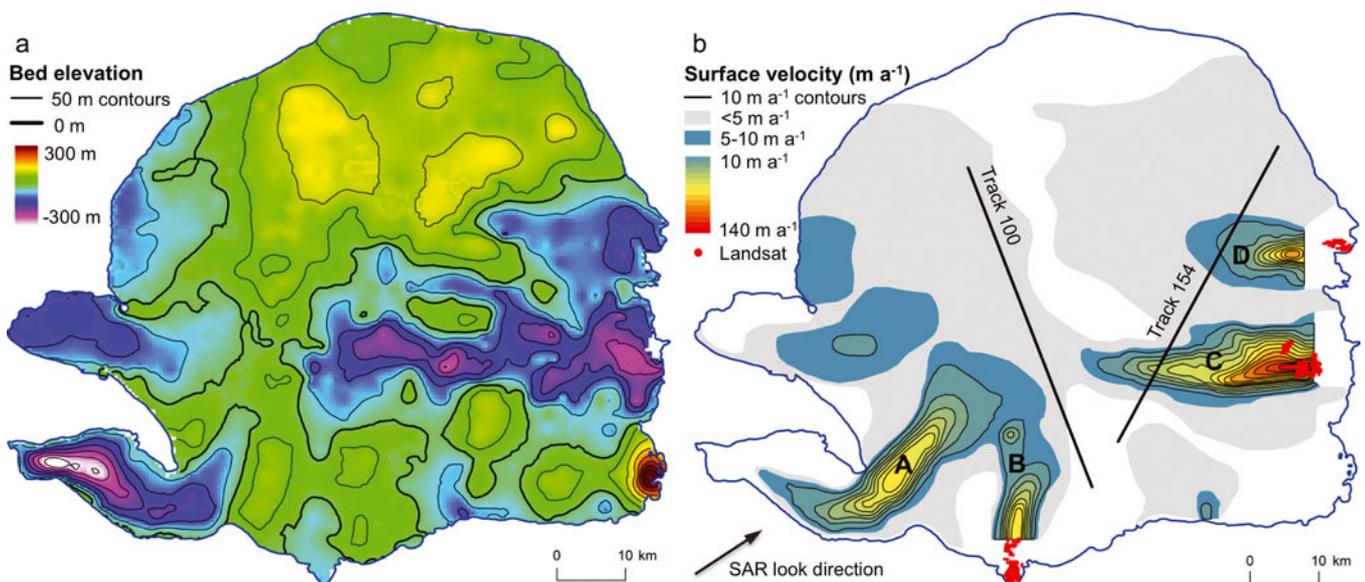
Fig. 2. (a) Bed topography and (b) surface velocities from Dowdeswell and others (2002). Bed topography was interpolated from a grid of airborne RES profiles (Fig. 4a), and surface velocities were derived from SAR interferometry of two ERS-1/2 scenes acquired on 23–24 September 1995. White areas show regions where interferometric velocities could not be retrieved. Red dots show locations where surface velocities were derived from Landsat image matching (Fig. 3c and d). Ice streams A–D are labeled with capital letters. Black lines show the ICESat tracks in Figures 5 and 6.
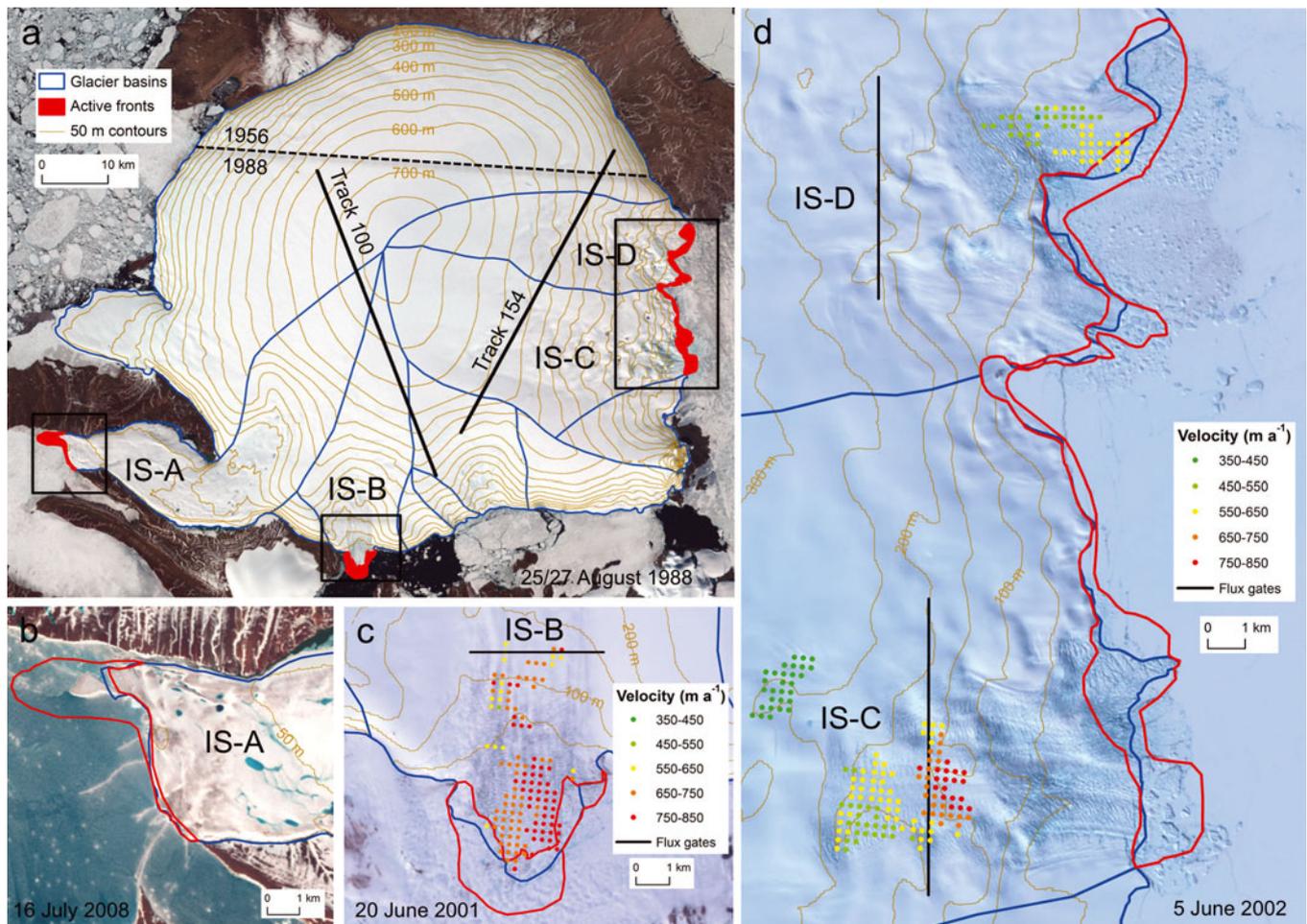
Fig. 3. (a) Surface topography and drainage basins of Academy of Sciences Ice Cap superimposed on a Landsat mosaic from 1988. The dashed black line shows the boundary between Russian topographic maps from 1956 and 1988. The solid black lines indicate the location of the ICESat tracks in Figures 5 and 6. Red areas show the maximum terminus fluctuations between 1962 and 2010 for the most active marine basins as observed by satellite imagery from Corona (1962 and 1979) and Landsat (1973, 1985, 1988, 1994, 2000–02 and 2008–10). The black frames indicate the location of the three Landsat insets over (b) ice stream A, (c) ice stream B and (d) ice streams C and D. Red polygons show the maximum terminus fluctuations corresponding to the red areas in (a). Color-coded dots show surface velocities from Landsat image matching of ice streams B (20 June 2001 to 9 July 2002), C (20 June 2001 to 5 June 2002) and D (12 July 2000 to 5 June 2002). The black lines are imaginary gates for calving flux estimation.

TERMINUS CHANGES

The large-scale dynamics of ice streams can be sensitive to changes in the terminus environment, both in terms of submarine ice melting and the buttressing effect of grounded ice tongues, ice shelves and sea ice. Marine glacier retreat is widespread over most of the High Arctic (Sharov, 2005; Błaszczyk and others, 2009) and can play a key role in the mass budget of marine ice caps (Dowdeswell and others, 2008; Moholdt and others, 2010a). We investigated terminus changes around Academy of Sciences Ice Cap by using multitemporal satellite imagery from Corona and Landsat, acquired between 1962 and 2010. The images were georeferenced to topographic maps, and terminus outlines were digitized for all visible ice streams in each image. Finally, a polygon was made around the minimum and maximum terminus extent of the four investigated drainage basins (Fig. 3).

Ice stream A has maintained a stable terminus position apart from a small tongue that has broken off during the last decade. The insignificant InSAR velocities (Fig. 2b) and the absence of surface crevassing (Fig. 3b) suggest that the front is largely stagnant. The other three ice-stream termini are much more dynamic, with frontal fluctuations of up to 1–2 km within the last five decades. Large tabular icebergs are present in many of the images, indicating partly floating tongues (Dowdeswell and others, 2002; Fig. 3). The extent of these tongues can vary considerably within 1 year, but they remain relatively stable over decadal time-spans due to short-lived ice-shelf formation and break-up. There are no clear temporal trends in the terminus fluctuations. We calculated a total marine glacier area loss of $5 \, km^2$ between 1988 and 2009, but there were several examples of both advance and retreat. Assuming an average ice thickness of 100 m at the termini, this corresponds to an ice volume loss rate of only $0.02 \, km^3 \, a^{-1}$, which is not significant for the ice-cap mass balance.

SURFACE ELEVATION CHANGES

Topographic maps of Severnaya Zemlya originate from Russian aerial imagery acquired in the 1950s and 1980s. According to the map sheets, the northernmost quarter of the ice cap was mapped in 1956, while the southern three-quarters originates from 1988 (Fig. 3a). The maps are at
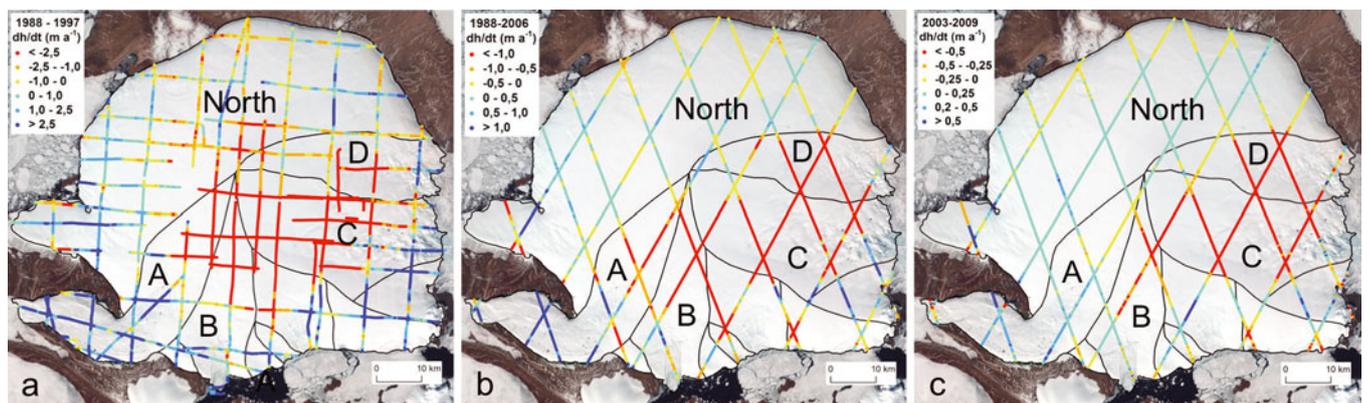
Fig. 4. Surface elevation-change rates along altimetry profiles for three different time-spans: (a) between the ~1988 DEM and the 1997 RES profiles, (b) between the ~1988 DEM and ICESat planes centered at 2006, and (c) between 2003 and 2009 from ICESat repeat-track planes. The DEM is based mainly on topographic maps from 1988, but a small section in the north derives from 1956 (Fig. 3a). Drainage basins are labeled A–D and North, in accordance with the basin names in Table 1.

1 : 200 000 with a contour interval of 40 m. We interpolated a continuous DEM at 50 m resolution from these contours using an iterative finite-difference interpolation technique (Hutchinson, 1989). This DEM was then compared directly with surface elevation profiles from airborne radio-echo sounding (RES) in 1997 and averaged Ice, Cloud and land Elevation Satellite (ICESat) laser altimetry from 2003 to 2009 to derive glacier elevation changes (Fig. 4a and b). A similar technique has previously been applied in a mass-balance study of glaciers in the Svalbard archipelago (Nuth and others, 2010). We also calculated elevation changes within the ICESat time period (Fig. 4c) using a regression technique that estimates surface slope and average elevation change, $\mathrm{d}h/\mathrm{d}t$, for planar surfaces that are fitted to 700 m long segments of tracks that are typically repeated within 100–200 m (Smith and others, 2009; Moholdt and others, 2010b). We used saturation-corrected elevation data from Release 531 of the GLA06 altimetry product (Zwally and others, 2002, 2010). Crossover points from radar altimetry missions can also be used to determine ice-cap elevation changes (Rinne and others, 2011), but the spatial resolution is typically too coarse to study ice-stream dynamics within length scales of ~10 km.

The three elevation-change maps in Figure 4 reveal similar spatial patterns. The most striking feature is the widespread thinning of basins C and D in the southeast of the ice cap, a pattern that has also been recognized previously (Sharov, 2010). These two basins have thinned by an average of 40 m since the topographic maps were constructed, and recently by an average rate of 1.1 m a^{-1} (2003–09). This is in sharp contrast to basin north, which has not changed significantly over the last three to five decades (Table 1). The relatively homogeneous pattern of elevation change in basin north over the periods 1956/88–2006 (DEM–ICESat) and 2003–09 (ICESat–ICESat) suggests that these datasets are of good quality. The 1956/88–1997 (DEM–RES) comparison is noisier due to a shorter time-span and the relatively coarse resolution of RES measurements.

Basins A and B show the most varied elevation changes. The dynamic mass flux at the equilibrium line of basin A must be larger than the balance flux, causing thinning in the upper parts and a corresponding thickening in the lower parts (Fig. 4a–c). This instability was much larger in the period 1988–2006 than for 2003–09, indicating glacier deceleration. The surge-like elevation change pattern is supported by the velocity field of the 1995 InSAR data

Table 1. Area, mass balance and inferred calving flux for each ice-cap drainage basin and time-span. The source datasets are topographic maps (1988*), ICESat laser altimetry (2003–09), SAR interferometry (1995) and Landsat imagery (2002–10 and 2000–02). Basins, elevation changes and surface velocities are shown in Figures 2–4. Calving rates for basins B–D in 1988–2006 and 2003–09 correspond to the mass balance multiplied by basin area. The total calving fluxes are not exactly equal to the geodetic mass balances, due to residual elevation changes in non-active drainage basins

Glacier basin	Area	Mass balance		Calving			
	2002–10	1988–2006	2003–09	1995	1988–2006	2000–02	2003–09
	km^2	m w.e. a^{-1}	m w.e. a^{-1}	Gt a^{-1}	Gt a^{-1}	Gt a^{-1}	Gt a^{-1}
Basin north	2380	0.03 ± 0.18*	0.07 ± 0.06	~0	~0	~0	~0
Basin A	710	0.14 ± 0.23	0.14 ± 0.09	~0	~0	~0	~0
Basin B	410	-1.13 ± 0.28	-0.23 ± 0.12	0.03	0.5	0.3	0.1
Basin C	830	-2.30 ± 0.23	-0.86 ± 0.09	0.37	1.9	1.9	0.7
Basin D	470	-1.57 ± 0.26	-1.11 ± 0.11	0.12	0.7	~0.7	0.5
Others	770	-0.29 ± 0.23	-0.02 ± 0.09	~0.1	~0.1	~0.1	~0.1
Ice cap total	5570	-0.55 ± 0.16	-0.19 ± 0.05	0.6	3.2	~3.0	1.4

*The northernmost part of basin north refers to a topographic map from 1956 (Fig. 3a).
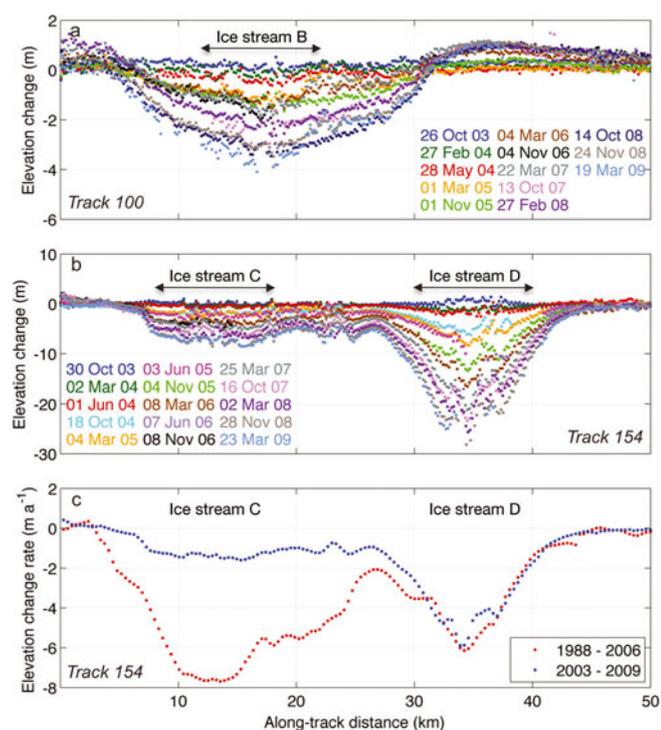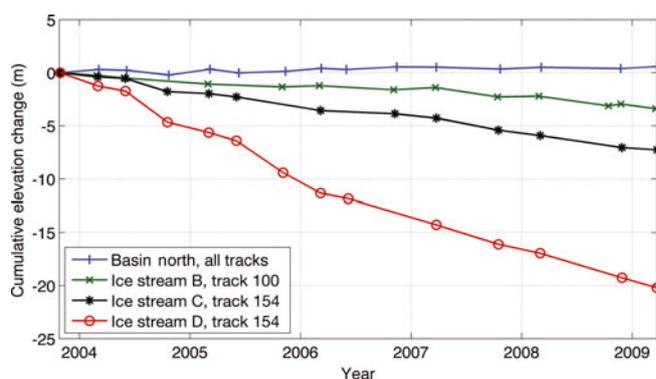
Fig. 5. (a, b) Cumulative elevation changes for all ICESat repeat passes along two selected reference tracks (100 and 154) that run across ice streams B–D. Black arrows indicate the central 10 km of each ice stream, which was used to determine the profile-wide temporal changes in Figure 6. (c) Average elevation-change rates along the same track as in (b) for the periods 1988–2006 (DEM–ICESat) and 2003–09 (ICESat–ICESat). The locations of tracks 100 and 154 are shown in Figure 3a. All ICESat elevation data have been corrected for the cross-track slope between near-repeat tracks.

(Fig. 2b). The upper parts of basin B have been thinning in both periods, but at a slower rate during the ICESat epoch. The steeper, lower parts of basin B are noisier, with no clear elevation-change patterns in either period.

The ICESat ground-tracks were repeated two to three times a year between 2003 and 2009, allowing derivation of temporal elevation change curves along selected profiles over rapidly changing surfaces (Fricker and others, 2007). Figure 5a and b show a time series of cumulative elevation changes along two ICESat reference tracks that cross the active zones of ice streams B–D. The most rapid dynamic thinning occurs in the center of the ice streams, where maximum downslope velocities are expected. The widths of the ice streams and the along-track patterns of thinning are consistent throughout the ICESat epoch. If we plot the average 2003–09 thinning rates against the 1988–2006 thinning rates for the same profile across ice streams C and D (Fig. 5c), it is evident that ice stream C must have slowed down markedly sometime before 2003. The thinning pattern of ice stream D is fairly similar for both periods, indicating sustained fast flow and a center-line thinning of >100 m since 1988, corresponding to ~20% of the ice thickness at that location.

We investigated potential temporal variations in thinning during 2003–09 by averaging all elevation-change measurements within the central 10 km of the ice streams for each repeat pass in Figure 5a and b. The results show that ice streams B–D have been thinning at fairly steady rates with no clear long-lived variations due to seasonality in glacier

Fig. 6. Cumulative average elevation changes for the central 10 km of ice streams B–D as sampled by the ICESat repeat tracks in Figure 5. The cumulative curve for basin north is determined from the campaign-wide average of all available repeat tracks that cover the basin (Fig. 4c). The locations of tracks 100 and 154 are shown in Figure 3.

dynamics or switches in the mode of flow (Fig. 6). The only slight trend is that the thinning of ice stream D appears to have slowed down since 2006. The seasonal signal from winter accumulation and summer ablation is too small to be detected over the rapidly changing ice streams, but can be identified in the basin-wide time series of elevation change in the slow-moving basin north (Fig. 6). The magnitude of these non-dynamical seasonal elevation changes is within ±0.5 m.

GEODETIC MASS BALANCE AND ERRORS

Our new ice-cap area estimate of $5570 \, km^2$ is not significantly different from the previous inventory ($5575 \, km^2$), which was made from 1988 Landsat imagery (Dowdeswell and others, 2002). Hence, we do not account for glacier area changes when calculating geodetic mass balances from our elevation-change measurements (e.g. Arendt and others, 2002). Spatial extrapolation of ICESat elevation change is typically carried out by assuming a relation between elevation change and altitude that is applied to the glacier hypsometry (e.g. Nuth and others, 2010). This relation fails for the most dynamically active drainage basins of Academy of Sciences Ice Cap, so we chose to calculate area-averaged elevation changes directly from the average elevation change within each basin. This can be justified through the homogeneous distribution of ICESat tracks across the ice cap (Fig. 4b and c). Basin-wide mass balances were then calculated by multiplying the averaged elevation change rates with an ice/water density ratio of 0.9 (Table 1).

Errors (1σ) in area-averaged mass balance (σ_{MB}) were estimated simply from

$$\sigma_{MB} = \sigma_{OBS}/\sqrt{n} + \sigma_{BIAS}$$

where σ_{OBS} is the precision of a single elevation-change measurement, n is the number of independent elevation-change measurements assuming a correlation length of 5 km (Moholdt and others, 2010b) and σ_{BIAS} is the potential bias in all elevation-change measurements. The precision of the DEM is unknown, but we expect it to be within 11 m (i.e. $\sigma_{OBS} = 11/18 \, m \, a^{-1} = 0.61 \, m \, a^{-1}$) since that is the standard deviation of the DEM−ICESat elevation differences in basin north, which should include both DEM errors and variations in glacier elevation change. The precision of ICESat

elevation-change rates has been estimated as $0.34 \, \mathrm{m \, a^{-1}}$ in similar terrain in Svalbard (Moholdt and others, 2010b). The temporal trend in ICESat inter-campaign biases is likely to be $<0.02 \, \mathrm{m \, a^{-1}}$ (Zwally and others, 2011). The DEM was corrected for a bias of 1.8 m as determined from ICESat over surrounding land surfaces, but we allowed for an error in this bias of 2 m (i.e. $\sigma_{BIAS} = 2/18 \, \mathrm{m \, a^{-1}} = 0.11 \, \mathrm{m \, a^{-1}}$) since the land morphology is different from the ice cap. The error due to unknown density changes in the firn pack is probably small since almost all mass loss is caused by glacier dynamics. Using these methods and assumptions, we estimate an ice-cap mass balance of $-0.55 \pm 0.16 \, \mathrm{m \, w.e. \, a^{-1}}$ ($-3.1 \, \mathrm{Gt \, a^{-1}}$) for 1988–2006 and $-0.19 \pm 0.05 \, \mathrm{m \, w.e. \, a^{-1}}$ ($-1.1 \, \mathrm{Gt \, a^{-1}}$) for 2003–09 (Table 1). The mass losses are dominated by basins B–D.

We did not calculate any mass balances for the 1988–97 period (DEM–RES) because of the large uncertainty of the RES surface-elevation data. The mean elevation difference at crossover points between RES profiles is $6.9 \pm 4.9 \, \mathrm{m}$ (Dowdeswell and others, 2002), while the corresponding precision of campaign-wise ICESat crossovers is better than 1 m (Moholdt and others, 2010b). The RES data are susceptible to elevation biases due to the retracking of the surface return, radar-signal penetration in dry snow/ice and local pressure fields that influence the pressure-altimeter recordings (Bassford, 2002; Moholdt, 2010). We adjusted all RES elevations by +9 m to account for a potential bias that we determined over basin north where elevation changes are expected to be small. Figure 4a should therefore only be used to interpret large-scale spatial patterns in elevation change.

CLIMATIC MASS BALANCE

Analysis and modeling of an ice-core record from the summit indicate that Academy of Sciences Ice Cap has been growing until modern times, with an average accumulation rate of $0.46 \, \mathrm{m \, w.e. \, a^{-1}}$ between 1956 and 1999 (Fritzsche and others, 2005). The whole ice core was cold, but meltwater percolation and refreezing were evident through most of the 60 m deep firn layer. Surface melting and ponding can also be seen in many of the summer Landsat scenes, especially at the lowermost elevations in basins A, C and D (Fig. 3). In situ mass-balance measurements and modeling conducted at the more southerly Vavilov Ice Cap (Fig. 1) indicate a slightly negative climatic mass balance of $-0.02 \, \mathrm{m \, w.e. \, a^{-1}}$ between 1974 and 1988, with an average equilibrium-line altitude of 500 m (Bassford and others, 2006). They found that 40% of the total net accumulation occurred as refreezing of meltwater in the firn pack, thus limiting the potential for meltwater to penetrate to the bed in the accumulation area.

In this study, we use basin north as an analogue for the climatic mass balance of the ice cap. This can be justified since the northern part of the ice cap seems to be dynamically inactive (Fig. 2b), with no significant mass loss from iceberg calving. The geodetic mass balances for basin north indicate a slightly positive climatic mass balance for both periods, but only the 2003–09 period is significantly positive (Table 1). Due to the small magnitude of the climatic mass-balance signal and the uncertainty in extrapolating it to the more dynamic basins, we simply set the climatic mass balance of the ice cap to a constant of $0 \, \mathrm{m \, w.e. \, a^{-1}}$ when calculating calving fluxes. This assumes

no strong directional gradients in climatic mass balance, similar to those observed on the ice caps of Austfonna in northeastern Svalbard (Schuler and others, 2007; Moholdt and others, 2010a) and Flade Isblink in northeastern Greenland (Rinne and others, 2011).

ICEBERG CALVING FLUX

The difference between geodetic and climatic mass balance has previously been used to estimate the calving flux of Kronebreen, Svalbard (Nuth and others, 2012). If the climatic mass balance and the mass change from terminus fluctuations are negligible, then the iceberg calving flux will simply equal the geodetic mass balance. The geodetic mass balance of basin A is slightly positive for all periods (Table 1). The terminus was dynamically stagnant in 1995 and has maintained a fairly stable position since the early 1960s. Hence, we conclude that iceberg calving is negligible for this basin despite the surge-like geometric-change pattern and the high upstream velocities in 1995. For the remaining ice streams (basins B–D), we estimate the calving flux by multiplying the area-averaged geodetic mass balances by their respective basin areas (Table 1). Assuming that the other slow-moving termini of the ice cap calve at a total rate of $\sim 0.1 \, \mathrm{Gt \, a^{-1}}$ (Dowdeswell and others, 2002), we obtain a total calving flux of $\sim 3.2 \, \mathrm{Gt \, a^{-1}}$ for 1988–2006 and $\sim 1.4 \, \mathrm{Gt \, a^{-1}}$ for 2003–09.

Most existing calving estimates in the Arctic are based on surface-velocity measurements across a fixed flux gate with known width and depth (e.g. Dowdeswell and others, 2008; Williamson and others, 2008; Błaszczyk and others, 2009). Dowdeswell and others (2002) used the lowermost extent of the 1995 InSAR velocities (Fig. 2b) to estimate the ice flux through gates with ice thicknesses determined from RES. They derived a total calving flux of $\sim 0.6 \, \mathrm{Gt \, a^{-1}}$, which is several times lower than the long-term estimates derived from basin-wide elevation changes. The InSAR-derived calving estimate can potentially be biased too low due to unresolved glacier movement perpendicular to the SAR look angle (Fig. 2b), but the elevation-change maps in Figure 4 do not suggest any major dynamic activity outside the four detected ice streams.

The Landsat-derived velocities from 2000–02 are restricted to the crevassed zones of ice streams B–D (Fig. 3c and d). Although these measurements lack the spatial coverage of the InSAR data, they have the advantage of capturing surface velocities close to the termini where calving occurs. If we assume the same flux gates as for the 1995 InSAR data, we can use the Landsat velocities to infer calving fluxes for the years 2000–02. Ice streams B and C have velocity data around their flux gates (Fig. 3c and d), so we used the average velocity within a 1 km buffer of each gate (671 and $685 \, \mathrm{m \, a^{-1}}$, respectively) to estimate calving fluxes (Table 1). Ice stream D does not have any data close to its flux gate, so we had to expand the buffer to 5 km and assume that the frontal velocities are representative of the upstream gate. All these flux estimates should be treated with caution since the Landsat velocity fields do not span the full width of the ice streams (Fig. 3c and d). It is likely that the gate-averaged velocities are slightly too high because the matching points are spatially biased towards the center of the ice streams (ice streams B and C) or the front (ice stream D) where velocities are expected to be higher. On the other hand, glacier acceleration might have widened the ice

streams with respect to the 1995 flux gates, thus allowing a larger ice flux and more calving. In any case, most of the ice flux is confined to the central bedrock troughs where the ice streams are thickest, so the error due to these unknown factors is likely to be $<0.5\,\mathrm{Gt\,a^{-1}}$ in total. We are therefore confident that there has been a sharp increase in calving between 1995 and 2000–02 ($\sim0.6\,\mathrm{Gt\,a^{-1}}$ versus $\sim3.0\,\mathrm{Gt\,a^{-1}}$). This is further confirmed by the independent calving estimates derived from elevation changes (Table 1).

DYNAMIC IMPLICATIONS

The results of this study highlight the temporal variability of iceberg calving as a consequence of ice-stream instability on a large Arctic ice cap. Ice-stream calving rates of up to $1\,\mathrm{Gt\,a^{-1}}$ are not unheard of in the Arctic archipelagos, but they are typically associated with short-lived advances and calving events caused by glacier surging (e.g. Dowdeswell and others, 1991). The ice streams of Academy of Sciences Ice Cap do not appear to fit into a simple surge or non-surge classification. Basin A is the only one that has a typical post-surge geometry, with a large low-gradient lobe at low elevations (Dowdeswell, 1986). The observed pattern of high-elevation thinning and low-elevation thickening could support the interpretation of a surge, but the total changes since 1988 are only on the order of $\pm30\,\mathrm{m}$, with no clear signs of surface crevassing. The terminus position has been stable since the 1960s, so the potential surge lobe must have formed before that.

Ice streams B–D were flowing relatively fast in 1995 (Fig. 2b), and surface velocities on the order of $50–100\,\mathrm{m\,a^{-1}}$ are only possible through basal sliding. Given that the beds of these ice streams lie mainly below sea level, it is likely that their bases are made up of deformable marine sediments that support semi-permanent sliding. Plumes of suspended sediment are sometimes observed in the waters in front of the termini in Landsat imagery. Oscillations in fast flow can be caused by changes in thermal or hydrological conditions at the bed or by changes in driving stresses. We do not have the data to investigate this, but our observations suggest that the dynamic regime of the ice cap is more complicated than the typical on/off switching associated with glacier surging. This is in line with a century-scale modeling study of the similar-sized Austfonna ice cap, which found that some basins exhibited oscillatory surge flow whereas others behaved like ice streams with time-variable fast flow (Dunse and others, 2011a).

Drainage of surface meltwater to the bed has been linked with glacier speed-up events on the Greenland ice sheet (Zwally and others, 2002). Recent studies have shown that these accelerations are mostly short-lived and do not contribute to increased calving (Sundal and others, 2011). We have no data on surface melting of Academy of Sciences Ice Cap, but the lack of seasonal variation in ice-stream thinning (Fig. 6) suggests that it is of relatively little importance for the large-scale dynamics of the ice cap. Submarine melting rates at the termini are not known, but could potentially be important if relatively warm water reaches the calving fronts (Holland and others, 2008). However, we have not observed any substantial retreat along the more stagnant ice fronts around the ice cap, indicating that submarine melting is probably small. The dynamic impact from terminus fluctuations is probably also small because the ice fronts have maintained a relatively stable position over the last ~50 years. The lack of clear external forcing mechanisms suggests that the observed dynamic instabilities of the ice cap are of an intrinsic nature rather than being linked to climate change.

Recent studies have shown that variations in ice-stream dynamics play a major role in the mass balance of the West Antarctic ice sheet (e.g. Joughin and Tulaczyk, 2002; Pritchard and others, 2009; Jenkins and others, 2010). Although much smaller in scale, Academy of Sciences Ice Cap shows similar patterns of ice-stream flow, with mass balance being determined largely by variability in glacier dynamics and calving. The timescales of ice-stream speed-ups and slowdowns are probably different between ice sheets and ice caps, but the processes that drive them may be similar. High Arctic ice caps can serve as an analogue for larger ice sheets, being much more manageable to model due to their smaller size and the easier acquisition of input data.

CONCLUSIONS

Academy of Sciences Ice Cap is highly dynamic, with a large temporal variability in ice-stream flow and calving. The mass balance of the ice cap during the last three decades is largely related to variations in calving from the three most active ice streams. The climatic mass balance of the ice cap is slightly positive or close to zero given the small rates of surface elevation change in non-active glacier basins. Elevation changes across the whole ice cap indicate an overall mass balance of $-3.06\pm0.86\,\mathrm{Gt\,a^{-1}}$ for 1988–2006 and $-1.05\pm0.25\,\mathrm{Gt\,a^{-1}}$ for 2003–09. The recent decrease in negative mass balance is mainly due to a slowdown of the largest ice stream.

Marine ice-terminus positions have remained stable to within $\pm2\,\mathrm{km}$ since the 1960s, probably because the ice streams tend to form floating tongues that break up intermittently into tabular icebergs (e.g. Williams and Dowdeswell, 2001). The ice-cap calving rate is therefore governed mainly by ice-stream flow. The three most active ice streams were all flowing much faster in 2000–02 than in 1995, leading to an increase in glacier calving from $\sim0.6\,\mathrm{Gt\,a^{-1}}$ to $\sim3.0\,\mathrm{Gt\,a^{-1}}$ over less than a decade. Recent elevation-change measurements from ICESat indicate that at least one of these ice streams has slowed down such that the current calving rate is $\sim1.4\,\mathrm{Gt\,a^{-1}}$. New and future satellite missions (e.g. CryoSat-2 and ICESat-2) will be essential for monitoring the future mass balance of the ice cap.

This study demonstrates that iceberg calving in the High Arctic is not necessarily a linear process with time. Academy of Sciences Ice Cap has been out of balance for several decades, unlike the short-term mass losses that are typical for surging glaciers. The observed ice-stream instabilities are also relevant for ice-sheet dynamics, calling for more research in order to understand the processes behind ice-stream flow variability.

REFERENCES

Arendt AA, Echelmeyer KA, Harrison WD, Lingle CS and Valentine VB (2002) Rapid wastage of Alaska glaciers and their contribution to rising sea level. *Science,* **297**(5580), 382–386 (doi: 10.1126/science.1072497)

Bassford RP (2002) Geophysical and numerical modelling investigations of the ice caps in Severnaya Zemlya. (PhD thesis, University of Bristol)

Bassford RP, Siegert MJ and Dowdeswell JA (2006) Quantifying the mass balance of ice caps on Severnaya Zemlya, Russian High Arctic. III: Sensitivity of ice caps in Severnaya Zemlya to future climate change. *Arct. Antarct. Alp. Res.,* **38**(1), 21–33

Błaszczyk M, Jania JA and Hagen JO (2009) Tidewater glaciers of Svalbard: recent changes and estimates of calving fluxes. *Pol. Polar Res.,* **30**(2), 85–142

Dowdeswell JA (1986) Drainage-basin characteristics of Nordaustlandet ice caps, Svalbard. *J. Glaciol.,* **32**(110), 31–38

Dowdeswell JA and Williams M (1997) Surge-type glaciers in the Russian High Arctic identified from digital satellite imagery. *J. Glaciol.,* **43**(145), 489–494

Dowdeswell JA, Hamilton GS and Hagen JO (1991) The duration of the active phase on surge-type glaciers: contrasts between Svalbard and other regions. *J. Glaciol.,* **37**(127), 388–400

Dowdeswell JA, Unwin B, Nuttall A-M and Wingham DJ (1999) Velocity structure, flow instability and mass flux on a large Arctic ice cap from satellite radar interferometry. *Earth Planet. Sci. Lett.,* **167**(3–4), 131–140

Dowdeswell JA and 10 others (2002) Form and flow of the Academy of Sciences ice cap, Severnaya Zemlya, Russian High Arctic. *J. Geophys. Res.,* **107**(B4), 2076 (doi: 10.1029/2000JB000129)

Dowdeswell JA, Benham TJ, Strozzi T and Hagen JO (2008) Iceberg calving flux and mass balance of the Austfonna ice cap on Nordaustlandet, Svalbard. *J. Geophys. Res.,* **113**(F3), F03022 (doi: 10.1029/2007JF000905)

Dunse T, Greve R, Schuler TV and Hagen JO (2011a) Permanent fast flow versus cyclic surge behaviour: numerical simulations of the Austfonna ice cap, Svalbard. *J. Glaciol.,* **57**(202), 247–259 (doi: 10.3189/002214311796405979)

Dunse T, Schuler TV, Hagen JO and Reijmer CH (2011b) Seasonal speed-up of two outlet glaciers of Austfonna, Svalbard, inferred from continuous GPS measurements. *Cryosphere Discuss.,* **5**, 3423–3453

Fitch AJ, Kadyrov A, Christmas WJ and Kittler J (2002) Orientation correlation. In Marshall D and Rosin PL eds. *Electronic Proceedings of the 13th British Machine Vision Conference, 2–5 September 2002, University of Cardiff.* CD-ROM, 133–142

Fricker HA, Scambos T, Bindschadler R and Padman L (2007) An active subglacial water system in West Antarctica mapped from space. *Science,* **315**(5818), 1544–1548 (doi: 10.1126/science.1136897)

Fritzsche D and 6 others (2005) A 275 year ice-core record from Akademii Nauk ice cap, Severnaya Zemlya, Russian Arctic. *Ann. Glaciol.,* **42**, 361–366 (doi: 10.3189/172756405781812862)

Gardner AS and 8 others (2011) Sharply increased mass loss from glaciers and ice caps in the Canadian Arctic Archipelago. *Nature,* **473**(7347), 357–360 (doi: 10.1038/nature10089)

Haug T, Kääb A and Skvarca P (2010) Monitoring ice shelf velocities from repeat MODIS and Landsat data – a method study on the Larsen C ice shelf, Antarctic Peninsula, and 10 other ice shelves around Antarctica. *Cryosphere,* **4**(2), 161–178 (doi: 10.5194/tc-4-161-2010)

Heid T and Kääb A (2012) Evaluation of existing image matching methods for deriving glacier surface displacements globally from optical satellite imagery. *Remote Sens. Environ.,* **118**, 339–355 (doi: 10.1016/j.rse.2011.11.024)

Holland DM, Thomas RH, de Young B, Ribergaard MH and Lyberth B (2008) Acceleration of Jakobshavn Isbræ triggered by warm subsurface ocean waters. *Nature Geosci.,* **1**(10), 659–664 (doi: 10.1038/ngeo316)

Hutchinson MF (1989) A new procedure for gridding elevation and stream line data with automatic removal of spurious pits. *J. Hydrol.,* **106**(3–4), 211–232

Jenkins A and 6 others (2010) Observations beneath Pine Island Glacier in West Antarctica and implications for its retreat. *Nature Geosci.,* **3**(7), 468–472 (doi: 10.1038/ngeo890)

Joughin I and Tulaczyk S (2002) Positive mass balance of the Ross ice streams, West Antarctica. *Science,* **295**(5554), 476–480 (doi: 10.1126/science.1066875)

Moholdt G (2010) Elevation change and mass balance of Svalbard glaciers from geodetic data. (PhD thesis, University of Oslo)

Moholdt G, Hagen JO, Eiken T and Schuler TV (2010a) Geometric changes and mass balance of the Austfonna ice cap, Svalbard. *Cryosphere,* **4**(1), 21–34 (doi: 10.5194/tcd-3-857-2009)

Moholdt G, Nuth C, Hagen JO and Kohler J (2010b) Recent elevation changes of Svalbard glaciers derived from ICESat laser altimetry. *Remote Sens. Environ.,* **114**(11), 2756–2767 (doi: 10.1016/j.rse.2010.06.008)

Nuth C, Moholdt G, Kohler J, Hagen JO and Kääb A (2010) Svalbard glacier elevation changes and contribution to sea level rise. *J. Geophys. Res.,* **115**(F1), F01008 (doi: 10.1029/2008JF001223)

Nuth C, Schuler TV, Kohler J, Altena B and Hagen JO (2012) Estimating the long-term calving flux of Kronebreen, Svalbard, from geodetic elevation changes and mass-balance modelling. *J. Glaciol.,* **58**(207), 119–133 (doi: 10.3189/2012JoG11J036)

Pritchard HD, Arthern RJ, Vaughan DG and Edwards LA (2009) Extensive dynamic thinning on the margins of the Greenland and Antarctic ice sheets. *Nature,* **461**(7266), 971–975 (doi: 10.1038/nature08471)

Rinne EJ and 6 others (2011) On the recent elevation changes at the Flade Isblink Ice Cap, northern Greenland. *J. Geophys. Res.,* **116**(F3), F03024. (doi: 10.1029/2011jf001972)

Scambos TA, Bohlander JA, Shuman CA and Skvarca P (2004) Glacier acceleration and thinning after ice shelf collapse in the Larsen B embayment, Antarctica. *Geophys. Res. Lett.,* **31**(18), L18402 (doi: 10.1029/2004GL020670)

Schuler TV, Loe E, Taurisano A, Eiken T, Hagen JO and Kohler J (2007) Calibrating a surface mass-balance model for Austfonna ice cap, Svalbard. *Ann. Glaciol.,* **46**, 241–248 (doi: 10.3189/172756407782871783)

Sharov AI (2005) Studying changes of ice coasts in the European Arctic. *Geo-Mar. Lett.,* **25**(2–3), 153–166 (doi: 10.1007/s00367-004-0197-7)

Sharov AI (2010) Satellite monitoring and regional analysis of glacier dynamics in the Barents–Kara region (SMARAGD). Joanneum Research Forschungsgesellschaft mbH, Graz, Austria

Smith BE, Fricker HA, Joughin JR and Tulaczyk S (2009) An inventory of active subglacial lakes in Anarctica dettected by ICESat (2003–2008). J. Glaciol., **55**(192), 573–595

Sole A, Payne T, Bamber J, Nienow P and Krabill W (2008) Testing hypotheses of the cause of peripheral thinning of the Greenland Ice Sheet: is land-terminating ice thinning at anomalously high rates? *Cryosphere,* **2**(2), 205–218 (doi: 10.5194/tc-2-205-2008)

Sundal AV, Shepherd A, Nienow P, Hanna E, Palmer S and Huybrechts P (2011) Melt-induced speed-up of Greenland ice sheet offset by efficient subglacial drainage. *Nature,* **469**(7331), 521–524 (doi: 10.1038/nature09740)

Williams M and Dowdeswell JA (2001) Historical fluctuations of the Matusevich Ice Shelf, Severnaya Zemlya, Russian High Arctic. *Arct. Antarct. Alp. Res.,* **33**(2), 211–222

Williamson S, Sharp M, Dowdeswell J and Benham T (2008) Iceberg calving rates from northern Ellesmere Island ice caps, Canadian Arctic, 1999–2003. *J. Glaciol.,* **54**(186), 391–400 (doi: 10.3189/002214308785837048)

Zwally HJ, Abdalati W, Herring T, Larson K, Saba J and Steffen K (2002) Surface melt-induced acceleration of Greenland ice-sheet flow. *Science,* **297**(5579), 218–222 (doi: 10.1126/science.1072708)

Zwally HJ and 7 others (2010) *GLAS/ICESat L1B Global Elevation Data V031, 20 February 2003 to 11 October 2009.* National Snow and Ice Data Center, Boulder, CO. Digitnal media

Zwally HJ and 11 others (2011) Greenland ice sheet mass balance: distribution of increased mass loss with climate warming; 2003–07 versus 1992–2002. *J. Glaciol.,* **57**(201), 88–102 (doi: 10.3189/002214311795306682)